Cell PRESS
Neuron
Article

A Positive Feedback Signal Transduction Loop Determines Timing of Cerebellar Long-Term Depression

Keiko Tanaka[1] and George J. Augustine[1,*]
[1]Department of Neurobiology, Duke University Medical Center, Box 3209, Durham, NC 27710, USA
*Correspondence: georgea@neuro.duke.edu
DOI 10.1016/j.neuron.2008.06.026

SUMMARY

Synaptic activity produces short-lived second messengers that ultimately yield a long-term depression (LTD) of cerebellar Purkinje cells. Here, we test the hypothesis that these brief second messenger signals are translated into long-lasting biochemical signals by a positive feedback loop that includes protein kinase C (PKC) and mitogen-activated protein kinase. Histochemical "epistasis" experiments demonstrate the reciprocal activation of these kinases, and physiological experiments—including the use of a light-activated protein kinase—demonstrate that such reciprocal activation is required for LTD. Timed application of enzyme inhibitors reveals that this positive feedback loop causes PKC to be active for more than 20 min, allowing sufficient time for LTD expression. Such regenerative mechanisms may sustain other long-lasting forms of synaptic plasticity and could be a general mechanism for prolonging signal transduction networks.

INTRODUCTION

One of the most remarkable properties of long-term synaptic plasticity is that these synaptic modifications last for hours or longer, yet are evoked by synaptic activity that lasts for only a few minutes or less (Artola and Singer, 1993; Ito, 2001; Malenka and Bear, 2004). In cerebellar Purkinje cells, long-term synaptic depression (LTD) is elicited by simultaneous activity at the parallel fiber (PF) and climbing fiber (CF) synapses that innervate cerebellar Purkinje cells (Linden, 1994; Ito, 2001). It is well established that LTD is initiated by second messengers, such as IP3 and Ca^{2+} (Sakurai, 1990; Crépel and Jaillard, 1991; Linden et al., 1991; Konnerth et al., 1992; Kasono and Hirano, 1994; Eilers et al., 1997; Khodakhah and Armstrong, 1997; Lev-Ram et al., 1997; Finch and Augustine, 1998; Inoue et al., 1998; Miyata et al., 2000; Wang et al., 2000a). However, while the intracellular concentration of these second messengers drops within a second after synaptic activity ends (Konnerth et al., 1992; Eilers et al., 1997; Finch and Augustine, 1998; Wang et al., 2000a; Okubo et al., 2004), LTD typically occurs tens of minutes later and lasts for hours (or longer). It is not yet known how these transient second messenger signals are propagated in time to produce a long-lasting depression of synaptic transmission.

A computational study, based on a general model of cellular signal transduction (Bhalla and Iyengar, 1999), proposed that the duration of LTD signaling is prolonged by a positive feedback loop (Kuroda et al., 2001). This positive feedback loop is thought to include several enzymes known to be involved in LTD, such as protein kinase C (PKC), mitogen-activated protein kinase (MAPK), and phospholipase A2 (PLA2) (Linden and Connor, 1991; Hartell, 1994; Linden, 1995; De Zeeuw et al., 1998; Kawasaki et al., 1999; Reynolds and Hartell, 2001; Leitges et al., 2004), and it is postulated that these enzymes mutually activate each other as shown in Figure 1A. This model predicts that the positive feedback loop is activated by second messengers, most notably Ca^{2+}, and causes a sustained activation of PKC, which then phosphorylates AMPA-type glutamate receptors to initiate LTD. This computational model is capable of replicating many of the basic properties of LTD, such as the associative requirement for simultaneous PF and CF synaptic activity (Kuroda et al., 2001). The model also is capable of reproducing the quantitative relationship between intracellular calcium concentration ($[Ca^{2+}]_i$) and LTD (Tanaka et al., 2007). Inhibition of PLA2, which should disrupt the postulated positive feedback loop, produces the predicted changes in the $[Ca^{2+}]_i$ dependence of LTD (Tanaka et al., 2007), suggesting that this loop acts downstream of Ca^{2+} to initiate LTD. However, it remains to be determined whether the positive feedback loop is actually required for LTD induction and, if so, whether it can produce the postulated prolonged activation of PKC.

In this study, we have directly tested the positive feedback hypothesis in several ways. Our results show that the reciprocal activation of PKC and MAPK, the main feature of the proposed positive feedback loop, is required for LTD. Further experimental analysis establishes that the positive feedback loop extends synaptic signaling in time, permitting a Ca^{2+} signal that decays within a second after synaptic activity ceases to be converted into a sustained activation of PKC that accounts for the protracted time course of LTD expression. Thus, our data provide direct evidence for a role for the positive feedback loop in LTD and provide a specific proposal for the time course of signaling events involved in LTD that may provide insights into other forms of long-term synaptic plasticity.

RESULTS

The goal of our study was to test the positive feedback loop model of LTD shown diagrammatically in Figure 1A. First, we

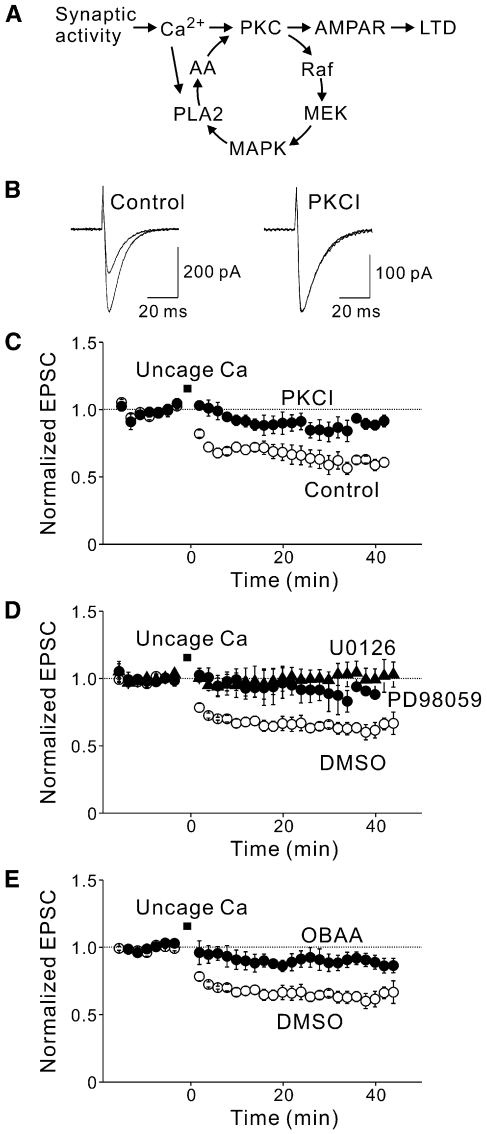

Figure 1. Ca^{2+} Is Upstream of PKC, MAPK, and PLA2

(A) Positive feedback loop model for LTD. AA, arachidonic acid; other abbreviations are given in the text.

(B) Superimposed PF-EPSCs recorded before and 20 min after uncaging Ca^{2+} in the absence (left) or presence (right) of intracellular PKCI (10 μM).

(C) Time course of LTD induced by uncaging Ca^{2+} (open circles, n = 7). LTD was blocked by including PKCI in the intracellular solution (closed circles, n = 6). PF-EPSC amplitudes are normalized to their mean preuncaging level.

(D and E) Ca^{2+}-triggered LTD also was blocked by the MAPK inhibitors PD98059 (100 μM; closed circles in [D], n = 5) and U0126 (20 μM; closed triangles in [D], n = 4) as well as the PLA2 inhibitor OBAA (5 μM; closed circles in [E], n = 5). DMSO, the solvent for these drugs, did not affect LTD (open circles in [D] and [E], n = 7).

Error bars in this and subsequent figures indicate ±1 SEM.

examined whether the enzymes proposed to participate in this loop—PKC, MAPK, and PLA2—are required downstream of Ca^{2+}. Next, we asked whether reciprocal activation of PKC and MAPK, which is predicted to form the positive feedback loop, is required for LTD. Finally, we asked whether the positive feedback loop leads to the prolonged activation of PKC that is postulated by the model.

PKC, MAPK, and PLA2 Work Downstream of Ca^{2+} during LTD

We used experiments analogous to genetic epistasis analysis (Lev-Ram et al., 1997) to determine whether PKC, MAPK, and PLA2 are required downstream of Ca^{2+}. Specifically, we asked whether the LTD produced by direct elevation of $[Ca^{2+}]_i$ could be blocked by inhibitors of PKC, MAPK, and PLA2. If the enzymes work downstream of Ca^{2+}, then these inhibitors should prevent Ca^{2+} from producing LTD; conversely, if the enzymes work upstream from Ca^{2+}, then the inhibitors should not block LTD.

For this purpose, we took advantage of previous observations that elevating $[Ca^{2+}]_i$ via photolysis of a caged Ca^{2+} compound is sufficient to induce LTD (Miyata et al., 2000; Tanaka et al., 2007). This Ca^{2+}-induced LTD shares a common signal transduction pathway with LTD induced by synaptic activity (Tanaka et al., 2007), justifying the use of this paradigm for analysis of the role of the signaling enzymes in LTD. $[Ca^{2+}]_i$ was elevated by using a spot of UV light, ~10 μm in diameter, to photolyze a caged Ca^{2+} compound (DMNPE-4) within Purkinje cell dendrites at the site where PFs were stimulated. LTD was evident as a reduction in the amplitude of excitatory postsynaptic currents evoked by electrical stimulation of PF axons (PF-EPSCs; Figure 1B, left). On average, PF-EPSCs were depressed by 37.8% ± 6.0% (n = 7) at 20–40 min after the elevation of $[Ca^{2+}]_i$ (Figure 1C). Introducing a PKC inhibitory peptide (PKCI; House and Kemp, 1987) into Purkinje cells caused LTD to be significantly smaller (13.0% ± 5.5%; p = 0.01; n = 6). Ca^{2+}-triggered LTD also was blocked by two small-molecule inhibitors of the MAPK pathway (Figure 1D). PD98059, which blocks this pathway by binding to the inactive form of the kinase upstream of MAPK, MEK (Alessi et al., 1995), reduced LTD to 10.7% ± 9.8% (n = 5). Likewise, U0126, which is a noncompetitive inhibitor of MEK (Favata et al., 1998), also reduced LTD to 1.2% ± 6.9% (n = 4). The reduction in LTD produced by each of these inhibitors was significantly different ($p < 0.05$) from the 36.3% ± 3.7% LTD (n = 7) measured in the presence of DMSO, the vehicle used to dissolve these inhibitors. Finally, OBAA, an inhibitor of PLA2 (Köhler et al., 1992), caused a reduction in LTD (9.7% ± 4.9%, n = 5) that also was significantly (p = 0.004) different from the LTD measured in the presence of the DMSO solvent (Figure 1E). Thus, inhibitors of all three enzymes blocked LTD induced by direct elevation of $[Ca^{2+}]_i$, indicating that these enzymes are required for LTD induced by Ca^{2+} and that they work downstream of Ca^{2+}, as predicted by the positive feedback loop model.

Reciprocal Activation of PKC and MAPK during LTD

The essence of the model is that PKC and MAPK mutually activate each other to create a positive feedback loop (Figure 1A). We tested this prediction by performing additional epistasis experiments that determined (1) whether PKC and MAPK activate each other during conditions that induce LTD and (2) whether such reciprocal activation of PKC and MAPK is required for LTD.

PKC Works Upstream of MAPK

We began by using biochemical assays to determine whether MAPK is activated during LTD and, if so, whether this is due to an upstream effect of PKC. To obtain sufficient tissue for these

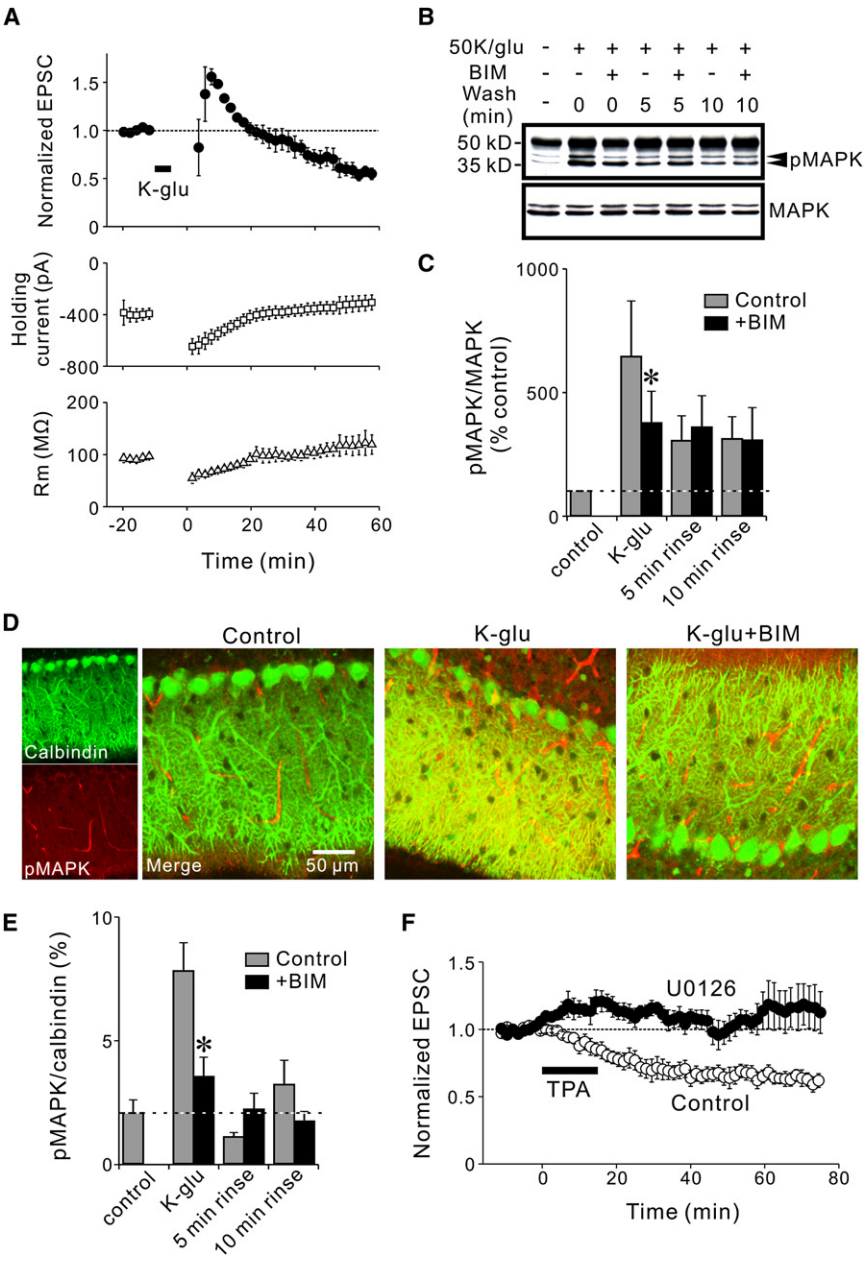

Figure 2. MAPK Is Activated during LTD and Is Required Downstream of PKC

(A) Time course of LTD induced by K-glu treatment (upper panel, n = 4). Holding current (middle panel) and membrane resistance (lower panel) were changed upon K-glu treatment but were gradually recovered.

(B) Immunoblots detecting phosphorylated MAPK (arrowhead in upper panel) and total MAPK (lower panel) in cerebellar slices. Bands at 50 kD in upper panel are immunoglobulin.

(C) Stimulation of slices with K-glu led to a sustained increase in phosphorylated MAPK (pMAPK) that was reduced by the PKC inhibitor, BIM (0.2 μM; n = 5–8).

(D) Images of cerebellar slices double-stained with antibodies against pMAPK (red) and calbindin (green).

(E) Quantification of pMAPK labeling in Purkinje cells (15 fields from three experiments).

(F) LTD induced by 0.5 μM TPA (open circles, n = 6) was blocked by 20 μM U0126 (closed circles, n = 5). Asterisks indicate significant difference ($p < 0.05$) between control and BIM treatment.

biochemical measurements, a "chemical LTD" protocol (Murashima and Hirano, 1999; Hirono et al., 2001; Endo and Launey, 2003), was used to induce LTD in cerebellar slices. This protocol involved treating the slices with 50 mM K^+—to mimic the depolarization and subsequent elevation of $[Ca^{2+}]_i$ that results from CF activity—and 10 μM glutamate (K-glu), to replicate the activation of metabotropic glutamate receptors that results from PF activity.

To validate this chemical stimulation paradigm, we asked whether the K-glu treatment induced an LTD of PF-EPSCs in cerebellar slices. K-glu treatment produced complex changes in Purkinje cell electrical properties and PF-EPSCs (Figure 2A). Immediately after K-glu treatment, the input resistance of the postsynaptic Purkinje cells was reduced by ~50%, and membrane holding current was proportionally increased. These changes presumably were due to the K-glu treatment causing a temporary activation of ion channels. During this time, EPSC amplitude was transiently increased; this increase could be a secondary consequence of the changes in passive membrane properties described above or could be due to activation of some short-term form of synaptic plasticity, such as posttetanic potentiation (Zucker and Regehr, 2002). After the membrane resistance and holding current of the Purkinje cells returned to basal levels, within 20–30 min after cessation of K-glu treatment, a gradual LTD of PF synaptic transmission was apparent. On average, PF-EPSCs were depressed by 32.3% ± 10.0% (n = 4) when measured 40–60 min after the K-glu treatment. These results establish that the K-glu treatment produces LTD in cerebellar slices and are in line with a previous report that K-glu treatment causes a day-long depression of miniature EPSC amplitude in cultured Purkinje cells (Murashima and Hirano, 1999).

We next asked whether this chemical LTD stimulus activated MAPK. Because it is well established that phosphorylation of MAPK results in activation of this protein kinase (Nishida and Gotoh, 1993; Cobb and Goldsmith, 1995), activation of MAPK was determined by measuring its degree of phosphorylation. K-glu treatment caused phosphorylation of MAPK in cerebellar slice lysates, and this activation of MAPK persisted for at least 10 min after the K-glu solution was removed (Figures 2B and 2C). Phosphorylation of MAPK was significantly ($p = 0.04$) reduced

by the cell-permeable PKC inhibitor bisindolylmaleimide I (BIM), indicating that MAPK activation during chemical LTD conditions at least partially requires PKC.

Immunohistochemistry next was used to identify the cellular location of MAPK activated by PKC. Purkinje cells were identified by staining with an anti-calbindin antibody (Jande et al., 1981; Nordquist et al., 1988), and activated MAPK was identified by staining with the same antibody used to measure MAPK phosphorylation in the biochemical experiments (Figure 2D, left). In control conditions, there was very little phosphorylation of MAPK; because of the predominance of anti-calbindin staining, Purkinje cells appeared green when images of the two labels were overlaid (Figure 2D). However, K-glu treatment increased MAPK phosphorylation in Purkinje cells, apparent as a yellow color in the overlaid images (Figure 2D). This activation of MAPK was particularly evident in the dendrites of the Purkinje cells. As was the case for MAPK phosphorylation measured biochemically in the entire slice (Figure 2C), phosphorylation of MAPK in Purkinje cells was blocked significantly ($p = 0.005$) by BIM (Figure 2E). These results indicate that MAPK is activated in Purkinje cells during chemical LTD conditions and that an upstream action of PKC is required for this activation of MAPK. These conclusions are consistent with previous demonstrations that MAPK is involved in LTD (Kawasaki et al., 1999) and that activation of PKC by the phorbol ester, TPA, increases MAPK phosphorylation (Endo and Launey, 2003; Ito-Ishida et al., 2006).

To determine whether this interaction between PKC and MAPK is required for LTD of PF synaptic transmission, we used TPA treatment to activate PKC. As previously reported (Linden and Connor, 1991; Endo and Launey, 2003; Kondo et al., 2005), TPA (0.5 μM) caused LTD, which was evident as a gradual reduction in PF-EPSC amplitude (Figure 2F). At 20–40 min after the end of TPA application, PF-EPSC amplitude was reduced by 33.0% ± 5.5% ($n = 6$) and did not recover over the duration of the recording. This LTD was blocked by the MAPK pathway inhibitor U0126 (−4.5% ± 7.4% reduction; $p = 0.002$; $n = 5$), indicating that MAPK works downstream of PKC. These results are consistent with observations made in cultured Purkinje cells (Endo and Launey, 2003). Taken together, our results demonstrate that (1) MAPK is activated in Purkinje cells during LTD, (2) this activation requires the upstream action of PKC, and (3) this interaction between PKC and MAPK is required for LTD induction.

MAPK Works Upstream of PKC

We next asked whether MAPK also works upstream of PKC, as predicted by the hypothesis, and began by using immunohistochemical imaging to determine whether PKC is activated during LTD. Translocation of PKC to the plasma membrane, a hallmark of PKC activation (Newton, 2001), was visualized by staining slices with an antibody against PKCα, a PKC isoform involved in LTD (Leitges et al., 2004). Because of background staining of adjacent cells, as well as the small diameter of Purkinje cell dendrites, it was not practical to image PKC translocation within dendrites. Instead, PKC translocation was measured in Purkinje cell bodies. PKC was present throughout these cell bodies in control conditions, evident as a uniform yellow-green color in overlaid images of PKCα and calbindin staining (Figure 3A, left). However, K-glu treatment caused PKC to translocate to the plasma membrane, evident as a yellow ring around the edges

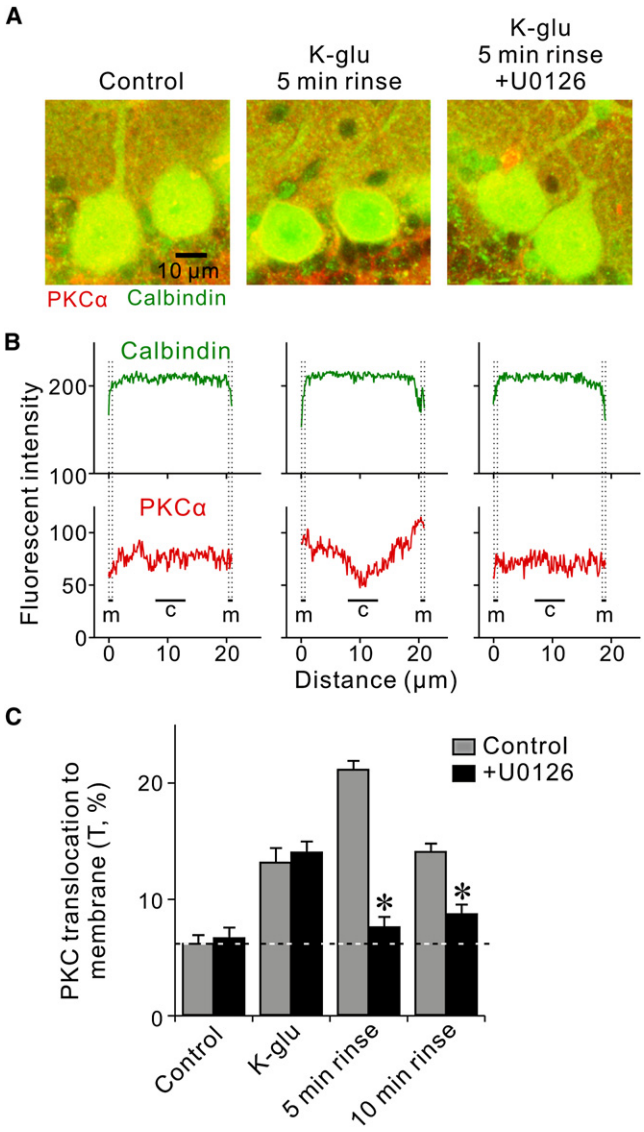

Figure 3. PKC Is Activated during LTD Induction

(A) Images of Purkinje cell soma in cerebellar slices double-stained with antibodies against PKCα (red) and calbindin (green).

(B) Line-scan profiles of calbindin (upper) and PKCα (lower) staining in Purkinje cell bodies. Intensity of PKCα staining at the membrane (m) and center of cell body (c) was measured.

(C) PKC translocation, quantified as $T = (m - c)/(m + c) \times 100$ (27–67 cells from six experiments). Asterisks indicate significant difference ($p < 0.05$) between control and U0126 (20 μM) treatment.

of Purkinje cell bodies (Figure 3A, middle). Translocation was quantified by using line-scan profiles to calculate the ratio of PKC staining at the membrane to that in the center, using calbindin staining to identify the Purkinje cell boundaries. Figure 3B illustrates such line scans, taken from the cells shown in the images of Figure 3A. PKC translocation occurred during the 5 min of K-glu treatment and was maintained for at least 10 min afterward (Figure 3C; $p < 0.001$). This persistent activation of PKC was blocked by treatment with U0126, although this drug had

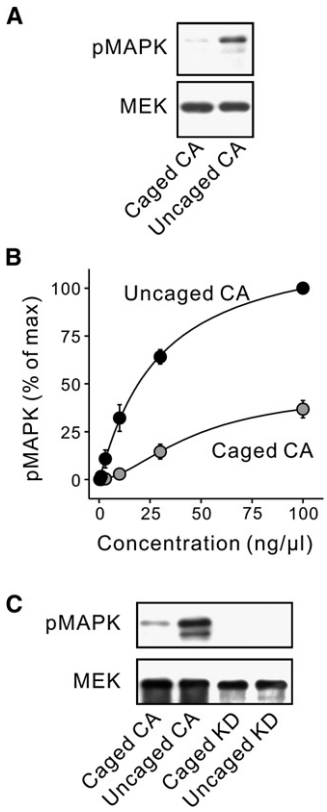

Figure 4. MAPK Is Activated by Uncaging MEK-CA

(A) Phosphorylation of purified MAPK protein by caged or uncaged MEK-CA (3 ng/μl) in vitro.

(B) Concentration-dependence of MAPK phosphorylation (pMAPK) by caged and uncaged MEK-CA (n = 5).

(C) MEK-KD (10 ng/μl) was unable to phosphorylate MAPK protein in vitro even after uncaging, while uncaged MEK-CA (10 ng/μl) strongly phosphorylated MAPK protein.

no effect during the K-glu treatment (Figures 3A and 3C). These results indicate that PKC activation in response to the chemical LTD stimulus consists of an initial, transient phase, perhaps due to the elevation of $[Ca^{2+}]_i$ by the K-glu treatment (Hockberger et al., 1989; Nishizuka, 1995; Newton, 2001), and a sustained phase that requires MAPK, perhaps due to the hypothetical positive feedback loop.

To determine whether this interaction between MAPK and PKC is required for LTD, we asked whether a PKC inhibitor could prevent LTD induced by direct activation of MAPK. Toward this goal, we produced a pseudophosphorylated, constitutively active form of MEK1 (MEK-CA) that phosphorylates/activates MAPK (Cobb and Goldsmith, 1995). Further, to provide temporal control over the activity of the MEK-CA, we covalently attached a NVOC-Cl caging group (Marriott et al., 2003). In vitro, the presence of the caging group greatly reduced the ability of MEK-CA to phosphorylate MAPK, while removing the cage via exposure to UV light (360 nm) greatly increased the ability of MEK-CA to phosphorylate MAPK (Figure 4A). Analysis of the relationship between MEK-CA concentration and MAPK phosphorylation indicated that uncaged MEK-CA was active at a ten times lower concentration than the caged MEK-CA: 30% of maximal MAPK phosphorylation occurred with 100 ng/μl caged MEK-CA, while the same degree of MAPK phosphorylation was produced by only 10 ng/μl uncaged MEK-CA (Figure 4B). In contrast, a caged, kinase-deficient form of MEK (MEK-KD) failed to phosphorylate MAPK after uncaging, even though uncaging parallel samples of MEK-CA did phosphorylate MAPK (Figure 4C). These results indicate that the caged MEK-CA permits light-controlled, and therefore temporally precise, activation of MAPK.

To determine the effect of activation of MAPK on PF synaptic transmission, we introduced the caged MEK-CA (1–2 μg/μl) into Purkinje cells through the patch pipette. PF-EPSC amplitude was constant during the 80 min (or longer) that caged MEK-CA was dialyzed into the Purkinje cell (Figure 5A), being reduced by only 6.2% ± 5.4% between 60 to 80 min after beginning dialysis of caged MEK-CA. This indicates that the caged MEK-CA had no effect on PF transmission. Using the same local uncaging approach described above for caged Ca^{2+} (Figure 1), the caged MEK-CA was photolyzed at a site where PFs were stimulated. This local photolysis of the caged MEK-CA caused a persistent reduction in PF-EPSC amplitude (Figure 5B). On average, PF-EPSC amplitude was reduced by 26.5% ± 2.9% (n = 23) when measured 20–40 min after uncaging MEK-CA. This degree of synaptic depression was not significantly different (p = 0.1) from the amount of LTD induced by uncaging Ca^{2+} (as in Figure 1C). Two results indicate that the LTD induced by uncaging MEK-CA was due to activation of MAPK, rather than being caused by some side product of the photolysis reaction or by the UV illumination. First, uncaging MEK-KD, instead of MEK-CA, caused no measurable depression (−0.4% ± 7.8%, n = 4, Figure 5B). Second, LTD induced by uncaging MEK-CA was blocked by U0126 (8.2% reduction in PF-EPSC amplitude at 30 min; n = 2).

To determine whether this LTD induced by activating MAPK shares the same downstream signaling pathways involved in conventional LTD, we asked whether induction of one form of LTD prevents any further depression of synaptic transmission by the other form of LTD. This type of occlusion experiment frequently has been used to determine whether forms of hippocampal synaptic plasticity share common signaling pathways (Gustafsson et al., 1987; Kauer et al., 1988; Muller et al., 1990; Cormier et al., 1993; Oliet et al., 1997) and has also been applied to LTD evoked by uncaging Ca^{2+} in Purkinje cells (Tanaka et al., 2007). When LTD was first elicited by uncaging MEK-CA, subsequent pairing of PF activity with depolarization of the Purkinje cell membrane potential (PF&ΔV; Crépel and Jaillard, 1991; Konnerth et al., 1992) produced no further depression of PF-EPSCs (Figure 5C; n = 4). The average reduction in PF-EPSC amplitude caused by uncaging MEK-CA was 30% ± 7%, while PF-EPSCs were subsequently slightly enhanced by 6% ± 7% following PF&ΔV (n = 4). Likewise, initially inducing LTD by PF&ΔV prevented any further depression of PF-EPSC amplitude by subsequent uncaging of MEK-CA (Figure 5D; n = 3). On average, paired stimulation reduced PF-EPSCs by 36% ± 11%, while uncaging MEK-CA reduced PF-EPSCs by only 6% ± 5% more (n = 3). In summary, regardless of which type of stimulus was presented first, the response to the second type of stimulus

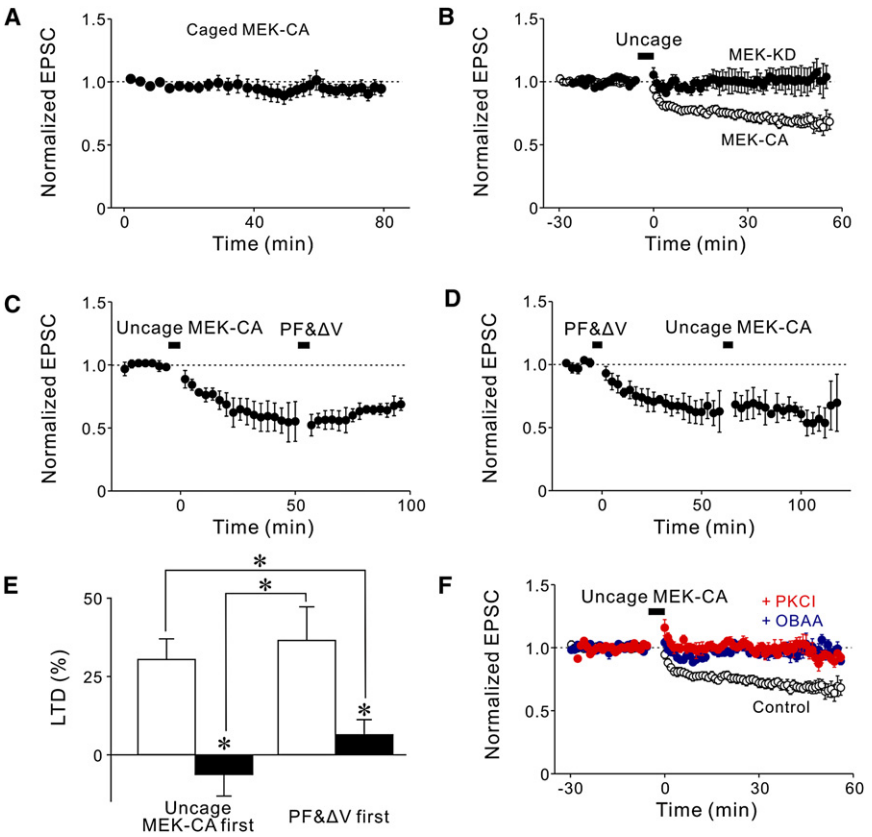

Figure 5. MAPK Activation by Uncaging MEK-CA Is Capable of Inducing LTD, which Requires PKC

(A) Measurement of EPSC amplitude during dialysis of caged MEK-CA into a Purkinje cell (n = 18). At time 0, whole-cell patch-clamp recording was established with an intracellular solution including caged MEK-CA. EPSC amplitude was normalized by dividing by the mean amplitude of EPSCs measured in each cell during the first 10 min of recording.

(B) LTD is induced by uncaging MEK-CA (n = 23) but not by uncaging MEK-KD (n = 4).

(C) Induction of LTD by uncaging MEK-CA prevents further depression by pairing PF stimulation with Purkinje cell depolarization (PF&ΔV, n = 4).

(D) The induction of LTD by PF&ΔV also prevents further depression by uncaging MEK-CA (n = 3).

(E) Summarized data of averaged reduction of PF-EPSC in occlusion experiments. Once LTD was induced by uncaging MEK-CA or PF&ΔV (open columns), subsequent LTD induction (closed columns) produced no further depression of PF-EPSCs. Asterisks indicate significant difference ($p < 0.05$).

(F) The LTD induced by uncaging MEK-CA is blocked by 10 μM PKCI (red, n = 6) or 5 μM OBAA (blue, n = 6). Control data are the same as in (B).

was significantly ($p < 0.05$) smaller than the response to the first stimulus type and also smaller than the response to the second type of stimulus alone (Figure 5E). This mutual occlusion indicates that LTD induced by uncaging MEK-CA and synaptically induced LTD share common signal transduction pathways. Thus, direct activation of MAPK in Purkinje cell dendrites is sufficient to cause LTD.

After characterizing the ability of uncaged MEK-CA to induce LTD, we could then use this tool to determine whether the LTD produced by direct activation of MAPK requires PKC. For this purpose, we uncaged MEK-CA in cells that also were dialyzed with the PKC inhibitor peptide, PKCI. The LTD resulting from uncaging of MEK-CA was completely blocked by dialysis of PKCI (Figure 5F). On average, the depression of PF-EPSCs in the presence of PKCI was −1.0% ± 2.4% (n = 5; $p < 0.001$), indicating that the interaction of MAPK with PKC is required for LTD. Further, LTD produced by direct activation of MAPK also requires PLA2: OBAA completely prevented uncaged MEK-CA from depressing PF-EPSCs (3.2% ± 2.0%; n = 6; $p < 0.001$). These results indicate that both PKC and PLA2 are required downstream of MAPK for LTD induction, as predicted by the model. Taken together, our results demonstrate that (1) PKC is activated in Purkinje cells during LTD, (2) this activation requires the upstream action of MAPK, and (3) this interaction between MAPK and PKC is required for LTD induction.

In summary, the chemical LTD experiments demonstrated the reciprocal activation of PKC and MAPK during LTD, and the experiments employing direct activation of PKC and MAPK demonstrated that such reciprocal activation is required to induce LTD. We thus conclude that the positive feedback loop is active during LTD and is required for LTD.

Positive Feedback Loop Sustains PKC Activation during LTD

Kinetic simulations predict that one of the main functions of the positive feedback loop is to translate the brief signals generated by synaptic activity into a sustained activation of PKC (Kuroda et al., 2001). We next tested this prediction by defining the time window when the PKC inhibitor, BIM, could prevent LTD. BIM alone did not affect PF-EPSCs (Figure 6A): PF-EPSCs measured 10–20 min after BIM application were 97% ± 7% (n = 4) of their amplitude measured prior to BIM application, which was not a significant change ($p = 0.69$). Applying PF&ΔV stimulation without BIM produced LTD (Figure 6B; see also Figure 5D). But if BIM was applied as late as 20 min after the PF&ΔV stimulus, LTD was reduced or eliminated (Figures 6C–6F). Even when BIM was applied at 20 min after the PF&ΔV stimulus, the amount of depression calculated 40–50 min after this stimulus was significantly ($p = 0.03$) smaller than in control experiments where BIM was not added. Applying BIM soon after LTD began (e.g., 10 min after the stimulus, Figure 6E) caused EPSC amplitude to partially recover, suggesting that the action of PKC was reversible at this time. Similar results were obtained by using another PKC inhibitor, Gö6976, demonstrating that the effects of BIM result from inhibition of PKC (Figure S1). However, applying BIM 30 min or later after the stimulus did not affect LTD (Figures 6G and 6H).

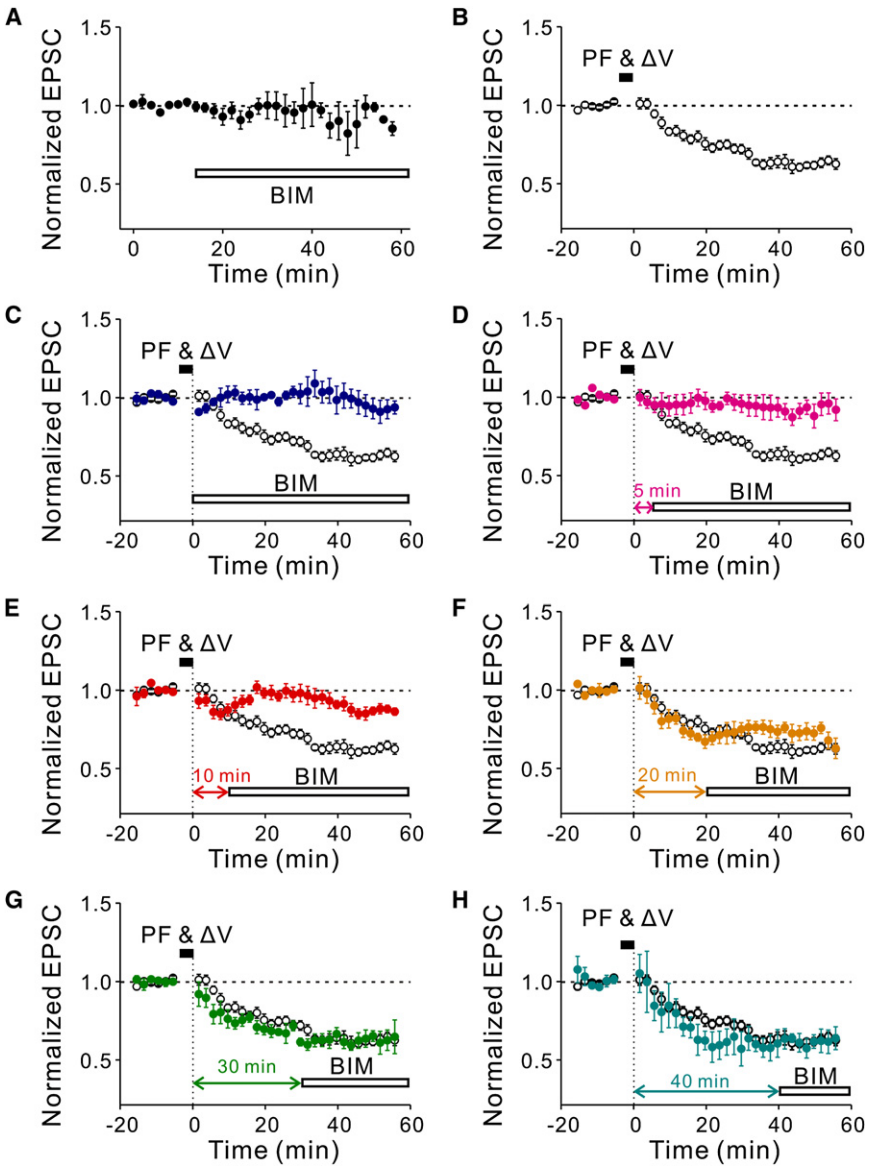

Figure 6. Sustained Activation of PKC Is Required to Induce LTD

(A) BIM treatment (0.5 μM) had no effect on the amplitude of PF-EPSCs (n = 4).

(B) LTD induced by PF&ΔV in control conditions (n = 9).

(C–H) The effect of external application of BIM at various times after PF&ΔV (black bars) on LTD (closed circles; n = 3–6). Control responses shown in (B), recorded in the absence of BIM, are overlaid for comparison in each panel (open circles).

The relationship between the time of BIM application and the degree of LTD impairment indicated that PKC remains active for at least 20–30 min after the end of the stimulus that induces LTD (Figure 8A). Thus, activation of PKC during LTD is prolonged, as predicted by the model.

To determine whether this prolonged activation of PKC requires the positive feedback loop, we disrupted this loop pharmacologically. For this purpose, we used the PLA2 inhibitor OBAA because the MAPK pathway inhibitor U0126 affected basal synaptic transmission (164% ± 7% of control; n = 4) while OBAA did not (Figure 7A; 95% ± 6%, n = 7). As was the case for BIM, OBAA was effective in reducing LTD even when applied 20–30 min after the end of the LTD-inducing stimulus (Figures 7C–7F). The relationship between the time of OBAA application and the degree of LTD impairment (Figure 8B) closely paralleled the relationship shown for BIM application in Figure 8A. We therefore conclude that the positive feedback loop is responsible for sustaining activation of PKC for at least the first 20–30 min after synaptic activity. This result also provides yet another indication that the loop is involved in LTD.

DISCUSSION

Previous computational and experimental results suggested that a positive feedback loop may initiate LTD by integrating postsynaptic Ca^{2+} signals (Kuroda et al., 2001; Tanaka et al., 2007). The results described in this paper establish that PKC and MAPK activate each other to create such a positive feedback loop and that the reciprocal activation of these enzymes is required to induce LTD. In addition, our results demonstrate that the loop is required to sustain activation of PKC for at least the first 20–30 min after synaptic activity.

Signaling Molecules Involved in the Positive Feedback Loop

Although experiments from several different experimental preparations previously implicated MAPK, PKC, and PLA2 in LTD (Linden and Connor, 1991; Hartell, 1994; Linden, 1995; De Zeeuw et al., 1998; Kawasaki et al., 1999; Reynolds and Hartell, 2001; Leitges et al., 2004), the targets of these enzymes during LTD induction had not been established aside from the phosphorylation of AMPA-type glutamate receptors (AMPARs) by PKC (Chung et al., 2003; Steinberg et al., 2006). Our experimental results indicate that these enzymes serve to reciprocally activate each other to form a positive feedback loop. The pair-wise interactions of these enzymes have been established by in vitro experimentation or by studies of signal transduction pathways in several cell types: MAPK directly phosphorylates and activates PLA2 (Lin et al., 1993), PLA2 produces AA (Clark et al., 1991), and AA binds to and activates PKC, alone or in conjunction with Ca^{2+} or diacylglycerol (Murakami and Routtenberg, 1985; Shinomura et al., 1991; Shirai et al., 1998; López-Nicolás et al., 2006). Although the mechanism involved is controversial, PKC-dependent activation of MAPK also has been observed in many types of cells (Marais et al., 1998; Corbit

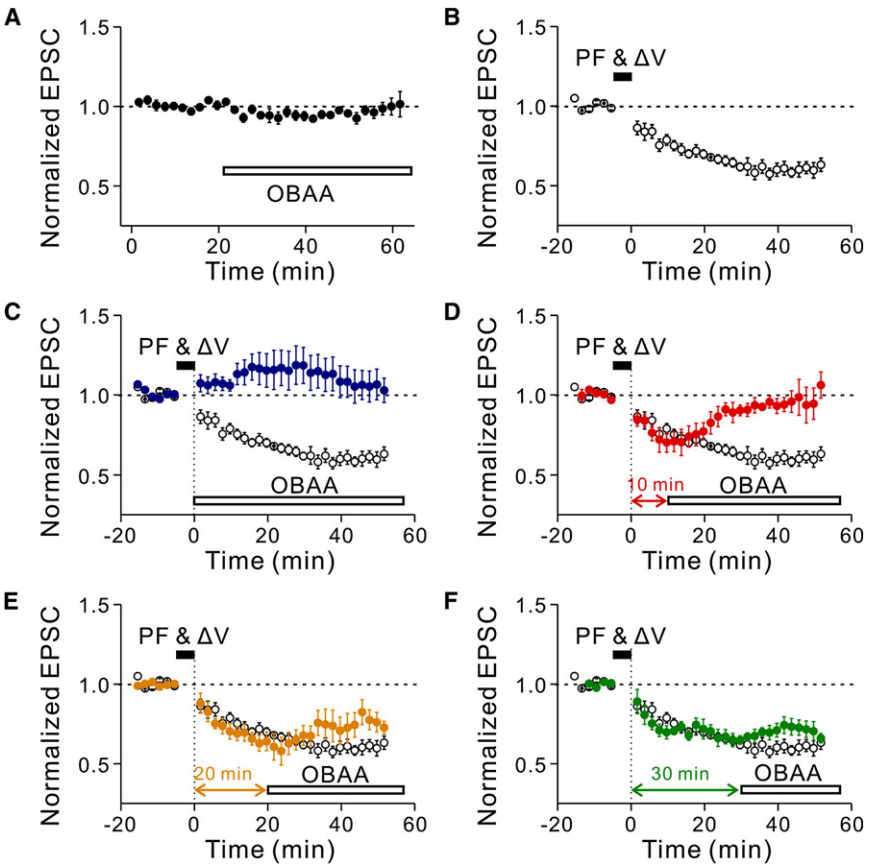

Figure 7. Sustained Activation of PLA2 Is Required to Induce LTD

(A) OBAA treatment (5 μM) had no effects on the amplitude of PF-EPSCs (n = 7).

(B) LTD induced by PF&ΔV in control conditions (n = 6).

(C–F) LTD measured after applying OBAA in the external solution at the indicated times (closed circles; n = 4–5) after PF&ΔV (horizontal bars). Control LTD shown in (B) is overlaid in each panel (open circles).

et al., 2003; Zheng et al., 2005; Wen-Sheng, 2006), including in Purkinje cells (Endo and Launey, 2003; Ito-Ishida et al., 2006). These interactions served as the basis for a theoretical study proposing that these enzymes can form a positive feedback loop (Bhalla and Iyengar, 1999). Our results provide direct experimental support for the notion that such a positive feedback loop can serve as a general mechanism for cellular signaling and specifically demonstrate that such interactions are important for LTD in Purkinje cells.

Kinetic modeling suggests that the main purpose of the positive feedback loop during LTD is to sustain activation of PKC (Kuroda et al., 2001). Our results provide several lines of experimental evidence supporting this suggestion. First, histochemical data indicated that PKC activity is sustained during conditions that evoke "chemical LTD" (Figure 3C). Second, biochemical data indicated that activation of MAPK also is sustained under such conditions (Figure 2C). Although our histological results (Figure 2E) suggest that MAPK activation in Purkinje cells may be more transient than indicated by the biochemical measurements, this discrepancy might be due to a sustained activation of MAPK that is too small and/or too localized to be detected in our histological experiments. (Even if MAPK activation were short-lived, the resultant phosphorylation-dependent activation of PLA2 should be sustained because subsequent dephosphorylation of PLA2 is very slow [Gordon et al., 1996].) Finally, timed application of pharmacological inhibitors indicated that activation of both PKC (Figure 8A) and PLA2 (Figure 8B) is sustained for at least 20 min after the end of the PF&ΔV stimulus that was used to induce LTD. These results are important because they demonstrate that the sustained activation of PKC by the positive feedback loop is required for LTD induction.

Time Course of Signal Transduction during LTD

Our studies provide information about the timing of reactions involved in LTD induction and expression. The 20–30 min time window we observed for the activity of the positive feedback loop during LTD is briefer than the 60–90 min predicted by the computational model of Kuroda et al. (2001). This indicates that mechanisms downstream of this loop sustain LTD earlier than expected. Thus, while our data largely confirm the computational model, they yield a new view of the signal transduction mechanisms underlying LTD induction, expression, and maintenance (Figure 9). We propose that synaptic activity transiently increases $[Ca^{2+}]_i$ (blue in Figure 9). Although the increase in $[Ca^{2+}]_i$ disappears within 1 s after synaptic activity ceases, activation of PKC and/or PLA2 by Ca^{2+} triggers the positive feedback loop. Once this loop is triggered, it causes PKC activity to be self-sustaining for at least 20–30 min (red in Figure 9). This time frame coincides with the time that LTD is gradually expressed (e.g., Figure 6B), indicating the cause of such slow development of LTD. Specifically, phosphorylation of PKC substrates, which presumably include AMPAR (Chung et al., 2003; Steinberg et al., 2006), during this time leads to internalization of AMPAR via clathrin-dependent endocytosis (Wang and Linden, 2000; Tanaka et al., 2007) and yields a gradual expression of LTD. At later times, more than 60–90 min after stimulation (green in Figure 9), synthesis of unknown new proteins is required to maintain LTD (Linden, 1996; Ahn et al., 1999). It is not yet clear what role, if any, the positive feedback loop plays in this late phase of LTD.

Between the time that the positive feedback loop is active (20–30 min) and the time that protein-synthesis-dependent mechanisms are involved (60–90 min), transmission at the PF synapse is maintained at a constant, depressed level (white in Figure 9). We presume that this phase of LTD arises from sustained changes in AMPAR trafficking. In Purkinje cells, the AMPARs involved in LTD are mainly composed of GluR2/3 subunits

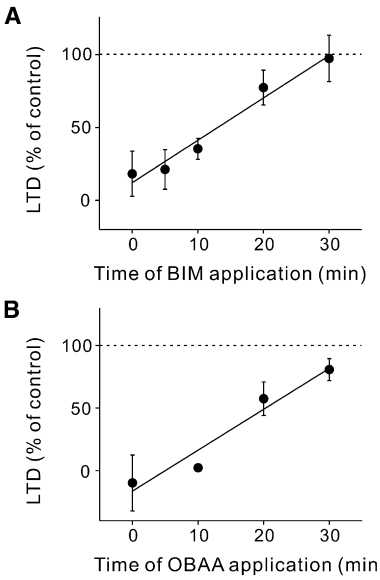

Figure 8. Sustained Activation of PKC and PLA2 Is Required for the LTD

(A and B) Mean LTD, measured 45–55 min after stimulation, are plotted as a function of the time when BIM (A) or OBAA (B) were applied. Data are normalized to LTD measured in control conditions, and lines indicate linear regression fits.

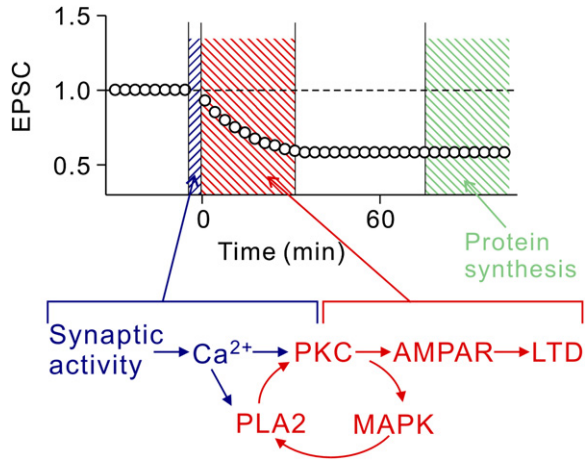

Figure 9. Model for Time Course of Signal Transduction Events Involved in LTD

LTD is initiated (blue) when synaptic activity generates short-lived second messengers such as Ca^{2+}, which leads to activation of the positive feedback loop (red) that causes LTD by phosphorylating AMPAR and leading to changes in AMPAR trafficking. At late times, synthesis of unknown new proteins leads to long-term maintenance of LTD (green).

(Ito, 2001; Chung et al., 2003), which are constitutively inserted and removed at many glutamatergic synapses (Bredt and Nicoll, 2003). Basal transmission at PF synapses is kept constant by maintaining a balance between insertion and removal of these AMPARs, because PF-EPSC amplitude is reduced when insertion of these AMPARs is blocked (Tatsukawa et al., 2006). Thus, the constant, reduced level of PF transmission produced between 20 to 60 min after stimulation probably is caused by AMPAR trafficking being maintained at a new equilibrium level with fewer surface AMPARs. The signaling mechanisms involved in establishing this new equilibrium remain to be determined.

When inhibitors of PKC or PLA2 were applied soon after LTD began, LTD was interrupted and EPSC amplitude recovered (Figures 6E, 7D, and S1B). These results indicate that LTD induction consists of at least two components that can be distinguished by the response to inhibitors of the positive feedback loop: one component causes a reversible depression of synaptic transmission, while the second component causes an irreversible depression. There seems to be a time-dependent progression from the reversible to irreversible components: under our experimental conditions, the reversible component was most evident when such inhibitors were applied 10 min after the LTD-inducing stimulus ended, while the irreversible component was more evident at later times. The molecular underpinnings of these two components remain to be determined; it is possible that the reversible component reflects reversible phosphorylation of AMPAR by PKC, with subsequent endocytosis of AMPAR, while the irreversible component may be some other reaction that results from positive feedback loop activity and causes LTD expression to be locked into an irreversible state. Our observation that inhibition of MAPK activation by U0126 completely blocked the LTD produced by TPA application (Figure 2F) suggests that MAPK has an additional role beyond activating PKC. Perhaps the reversible component reflects internalization of AMPAR caused by PKC-dependent phosphorylation, while MAPK activity is responsible for subsequent conversion of AMPAR trafficking into an irreversible state. Such an arrangement may account for the observation that PLA2 activation prolongs the duration of LTD, converting a short-term synaptic depression into LTD (Linden, 1995).

Although LTD is expressed progressively over time, the precise time course of LTD expression varies according to the type of stimulus and stimulus intensity (Ito, 2001). Even in our experiments, there were some stimulus-dependent differences in LTD time course: LTD induced by uncaging Ca^{2+} often reached a steady state within 5–10 min (Figure 1), while LTD induced by PF&ΔV (Figures 7 and 8) or K-glu treatment (Figures 2 and 3) was more gradual and reached a maximum over 20–30 min. Kinetic simulations predict that such stimulus-dependent variability arises from the efficacy of the stimulus in activating the positive feedback loop (Kuroda et al., 2001). Our refinement of the positive feedback model postulates that PKC activity need not be sustained after LTD expression is maximal; this may account for the observation of Tsuruno and Hirano (2007) that sustained PKC translocation cannot be observed in cultured Purkinje cells after the time that LTD is maximal.

Significance of the Positive Feedback Loop

The positive feedback loop was first postulated to serve as a bistable switch that allows brief stimuli to produce sustained activation of protein kinases (Bhalla and Iyengar, 1999). In Purkinje cells, rises in $[Ca^{2+}]_i$ associated with synaptic activity are short-lived (Konnerth et al., 1992; Eilers et al., 1997; Finch and Augustine, 1998; Wang et al., 2000a) and are limited in time by the activity of highly expressed Ca^{2+}-binding proteins and Ca^{2+} pumps

(Baba-Aissa et al., 1998; Hartmann and Konnerth, 2005). Thus, the bistable character of this loop effectively serves as a temporal integrator that translates brief Ca^{2+} signals into the long-lasting activation of PKC that is required for LTD. Bistability arising from positive feedback loops has also been proposed as a mechanism for regenerative spatial propagation of signals from the plasma membrane to the nucleus (Markevich et al., 2006). Although LTD is known to spread from active PF synapses to inactive ones (Wang et al., 2000b; Reynolds and Hartell, 2000), it is unlikely that the bistable properties of the PKC/MAPK/PLA2 positive feedback loop are responsible for this spread, because the positive feedback loop works downstream of Ca^{2+}, and it is known that LTD cannot spread beyond the site of $[Ca^{2+}]_i$ elevation (Tanaka et al., 2007). However, it remains possible that the positive feedback loop could be involved in signaling between active synapses and the nucleus during LTD (Linden, 1996).

Similar regenerative mechanisms may also serve as temporal integrators to maintain other forms of long-lasting synaptic plasticity. One prominent example has been well established for long-term potentiation of the Schaffer collateral synapse in the hippocampus. Here, a brief Ca^{2+} signal in postsynaptic pyramidal cells (Malenka et al., 1992; Petrozzino et al., 1995; Yang et al., 1999) leads to autophosphorylation of Ca^{2+}/calmodulin-dependent protein kinase II (CaMKII), a regenerative mechanism that yields the sustained activation of this kinase that is required for induction and maintenance of LTP (Lisman and Goldring, 1988; Giese et al., 1998; Lisman et al., 2002; Atkins et al., 2005; Sanhueza et al., 2007). Although CaMKII is also known to participate in cerebellar LTD (Hansel et al., 2006), it is not yet known whether it serves a regenerative function as in pyramidal cells. A second example can be found in a form of long-term synaptic facilitation that is important for long-term memory in *Aplysia*. This synaptic facilitation requires the self-perpetuating activation of a translational regulator, cytoplasmic polyadenylation element binding protein, that stabilizes a late phase of facilitation (Si et al., 2003; Bailey et al., 2004). Given that most forms of long-term synaptic plasticity are initiated by brief Ca^{2+} signals (Malenka et al., 1992; Yang et al., 1999; Franks and Sejnowski, 2002; Bonsi et al., 2004; Gall et al., 2005; Nevian and Sakmann, 2006; Humeau and Luthi, 2007), it is possible that regenerative mechanisms could be a common means of sustaining long-term synaptic plasticity.

EXPERIMENTAL PROCEDURES

Patch-Clamp Recording

Whole-cell patch-clamp recordings were made from Purkinje cells as described previously (Miyata et al., 2000; Wang et al., 2000b). Sagittal slices (200 μm) of cerebella from 14- to 21-day-old mice were bathed in extracellular solution containing (in mM) 125 NaCl, 2.5 KCl, 1.3 Mg_2Cl, 2 $CaCl_2$, 1.25 NaH_2PO_4, 26 $NaHCO_3$, 20 glucose, and 0.01 bicuculline methochloride (Tocris). TPA, PD98059, U0126, BIM (all from Calbiochem), or OBAA (Tocris) were added into the extracellular solution as indicated. When inducing "chemical LTD," an extracellular solution containing high K^+ (50 mM) and glutamate (10 μM) was applied under current-clamp conditions. Patch pipettes (resistance 3–5 MΩ) were filled with (in mM) 130 potassium gluconate, 2 NaCl, 4 $MgCl_2$, 4 Na_2-ATP, 0.4 Na-GTP, 20 HEPES (pH 7.2), and 0.25 Ca^{2+} indicator (Oregon Green 488 BAPTA-1, Molecular Probes) or EGTA. When LTD was induced by uncaging Ca^{2+}, 10 mM caged Ca^{2+} compound (DMNPE-4, gift from Dr. Graham Ellis-Davies) and 5 mM $CaCl_2$ were added into the internal solution (Tanaka et al., 2007). For the experiments using caged MEK proteins, caged MEK-CA or MEK-KD (1–2 mg/ml) were added into the internal solution along with dextran-conjugated fluorescein (Molecular Probes), to monitor the dialysis of intracellular solutions into Purkinje cells. In some experiments, PKCI (Sigma) was added into the internal solution.

EPSCs were evoked in Purkinje cells (holding potential of −70 mV) by activating PFs with a glass stimulating electrode on the surface of the molecular layer. PF-EPSCs were acquired and analyzed using LTP software (W.W. Anderson, University Bristol, UK; Anderson and Collingridge, 2001). To evoke LTD by electrical stimulation (PF&ΔV), PF stimuli were paired with Purkinje cell depolarization (0 mV, 200 ms) 300 times at 1 Hz. Data were accepted if the series resistance changed less than 20%, input resistance was greater than 80 MΩ, holding current changed less than 5%, and Ca^{2+} levels returned to baseline following photolysis of caged Ca^{2+}. Uncaging neither Ca^{2+} nor MEK proteins changed the input resistance or holding current, and UV illumination in the absence of caged compound did not affect PF synaptic transmission (Tanaka et al., 2007).

To evaluate the effect of applying BIM or OBAA at different times on the LTD induced by PF&ΔV (Figures 6 and 7), we measured the mean amount of depression at 45–55 min after LTD induction. The values used in Figure 8 were calculated as the percentage of depression in the presence of inhibitors divided by the amount of depression measured at this same time period in control conditions.

Live Cell Imaging and Photolysis of Caged Compounds

The procedures described previously (Tanaka et al., 2007) were used to image fluorescent dyes and to photolyze caged compound. Cells were dialyzed with a solution containing Oregon Green 488 BAPTA-1 and DMNPE-4 or a solution containing fluorescein dextran and caged MEK protein. The set-up described by Wang and Augustine (1995) was used to uncage Ca^{2+} or MEK. UV light (351–364 nm) from an argon ion laser (Coherent model 305) was delivered to the slice, via an optical fiber and an Olympus 40× water-immersion objective, to make a light spot with a half-width of 5–10 μm that was focused on the primary or secondary dendrites of a Purkinje cell. Photolysis was accomplished via a train of brief UV light flashes (5 ms duration, 1 Hz) that was controlled by an electronic shutter. For uncaging Ca^{2+}, the train was 90 s in duration, and the total UV energy applied was 300 μJ. For uncaging MEK, the duration and total energy were 5 min and 900 μJ, respectively.

Immunoblotting and Immunohistochemistry

Primary antibodies used for immunoblotting and immunohistochemistry were monoclonal anti-MAPK, monoclonal anti-phosphorylated MAPK (Cell Signaling Technology), monoclonal PKCα (BD Transduction Laboratories), and polyclonal anti-calbindin (Sigma). Secondary antibodies were horseradish peroxidase (HRP)-conjugated anti-mouse IgG, Cy5-conjugated anti-mouse IgG (Jackson ImmunoResearch Laboratories), and FITC-conjugated anti-rabbit IgG (Invitrogen).

Cerebellar slices were incubated for 30 min in normal ACSF, transferred to K-glu solution for 5 min, and then washed in normal ASCF for 0–10 min. Inhibitors were added for the entire duration of the experiment. For immunoblotting, slices were lysed in a RIPA buffer containing (in mM) 150 NaCl, 50 Tris (pH 8), 1% NP-40, 0.5% deoxycholate, 0.1% SDS, 1% aprotinin, 1 AEBSF, 5 NaF, 1 orthovanadate, 12 glycerophosphate, and 1 pyrophosphate tetrabasic decahydrate. After homogenization and sonication, samples were centrifuged to remove cell debris. A part of the supernatant was directly applied into SDS-PAGE to detect total amount of MAPK. The rest of the supernatant was used to immunoprecipitate phosphorylated MAPK by using an immobilized phosphorylated MAPK antibody (Cell Signaling Technology). The immunoprecipitate was suspended in SDS-PAGE sample buffer and applied into SDS-PAGE to detect phosphorylated MAPK by immunoblotting. To quantify MAPK phosphorylation, band intensities were measured by Igor Pro (Wave Metrics, Inc), and the ratio of phosphorylated MAPK to total MAPK was then calculated.

For immunohistochemistry, slices were fixed with 4% paraformaldehyde at 4°C, blocked in 5% normal goat serum in phosphate-buffered saline, and then incubated in primary antibodies overnight at 4°C. After several washes, slices were incubated in secondary antibodies for 3 hr at room temperature. Images

were acquired by a Leica TCS SP2 laser-scanning confocal microscope (Leica). Quantification of phosphorylated MAPK in Purkinje cells and PKCα membrane translocation were performed by Photoshop (Adobe) and Igor Pro. To compare phosphorylated MAPK, a threshold level of fluorescence was subtracted from all images of phosphorylated MAPK and calbindin. In these subtracted images, the number of pixels stained by both antibodies ($P_{pMAPK\&cal}$) and those stained by calbindin (P_{cal}) were counted, allowing the percentage ($P_{pMAPK\&cal}/P_{cal} \times 100$) to be calculated for each image. To quantify PKCα membrane translocation, intensity of PKCα staining was measured along a line 2 μm in width across the Purkinje cell soma, as shown in Figure 3B.

Construction and Characterization of Caged, Constitutively Active MEK

Recombinant glutathione-S-transferase-fused MEK1 was purified from *E. coli* by using glutathione sepharose (Amersham Biosciences). MEK-CA was a double mutation of serine residues 218 and 222 to glutamic acid, while MEK-KD was a single mutation of asparatic acid 208 to alanine (Cowley et al., 1994; Okazaki and Sagata, 1995). Purified MEK protein was caged according to a protocol described previously (Marriott et al., 2003) to cage actin-binding proteins. In brief, purified MEK protein, which was dialyzed in PBS and adjusted to ~pH 9.0 via the addition of $NaHCO_3$, was incubated with a 10-fold molar excess of the amino-directed protein-caging compound, 4,5-dimethoxy-2-nitrobenzyl chloroformate (NVOC-Cl, Sigma), in the dark for 30 min at 4°C. The unbound NVOC was removed by centrifugation at 15,000 rpm for 5 min followed by desalting through a PD-10 column (Amercham Biosciences). Final concentrations of MEK and NVOC were determined by a commercial protein assay (Bio-Rad) and OD_{360} measurements (OD360 = 5000 M^{-1} cm^{-1}), respectively. The labeling ratio typically ranged from 5 to 7 NVOC-Cl per MEK molecule. MEK binds to MAPK via its MAPK-binding domain, which includes three lysine residues important for this interaction (Tanoue and Nishida, 2003). We suspect that these lysine residues are masked by NVOC labeling and unmasked by UV photolysis.

To examine the activity of caged or uncaged MEK, in vitro assays of MAPK phosphorylation were performed. Caged MEK was photolyzed by 360 nm UV light from a transilluminator for 5 min. Caged or uncaged MEK was mixed with recombinant MAPK and ATP in kinase buffer (Cell Signaling Technology) and incubated for 30 min at 30°C. The kinase reaction was terminated by adding SDS-PAGE sample buffer. Samples were applied into SDS-PAGE, and phosphorylated MAPK was detected by immunoblotting with a phospho-MAPK antibody.

Statistical Analysis

Statistical differences were determined by paired comparisons with the Student's t test.

SUPPLEMENTAL DATA

The Supplemental Data can be found with this article online at http://www.neuron.org/cgi/content/full/59/4/608/DC1/.

ACKNOWLEDGMENTS

We thank G. Ellis-Davies for providing DMNPE-4 and K. Berglund, N. Calakos, Q. Cheng, I. Gotoh, M. Kawato, F. Santamaria, and R. Yasuda for comments on this paper. This work was supported by NIH grants, a Human Frontier Science Program grant, a postdoctoral fellowship from the Japan Society for the Promotion of Science, and a PRESTO grant from Japan Science and Technology Agency.

Accepted: June 27, 2008
Published: August 27, 2008

REFERENCES

Ahn, S., Ginty, D.D., and Linden, D.J. (1999). A late phase of cerebellar long-term depression requires activation of CaMKIV and CREB. Neuron *23*, 559–568.

Alessi, D.R., Cuenda, A., Cohen, P., Dudley, D.T., and Saltiel, A.R. (1995). PD 098059 is a specific inhibitor of the activation of mitogen-activated protein kinase kinase *in vitro* and *in vivo*. J. Biol. Chem. *270*, 27489–27494.

Anderson, W.W., and Collingridge, G.L. (2001). The LTP program: a data acquisition program for on-line analysis of long-term potentiation and other synaptic events. J. Neurosci. Methods *108*, 71–83.

Artola, A., and Singer, W. (1993). Long-term depression of excitatory synaptic transmission and its relationship to long-term potentiation. Trends Neurosci. *16*, 480–487.

Atkins, C.M., Davare, M.A., Oh, M.C., Derkach, V., and Soderling, T.R. (2005). Bidirectional regulation of cytoplasmic polyadenylation element-binding protein phosphorylation by Ca^{2+}/calmodulin-dependent protein kinase II and protein phosphatase 1 during hippocampal long-term potentiation. J. Neurosci. *25*, 5604–5610.

Baba-Aissa, F., Raeymaekers, L., Wuytack, F., Dode, L., and Casteels, R. (1998). Distribution and isoform diversity of the organellar Ca^{2+} pumps in the brain. Mol. Chem. Neuropathol. *33*, 199–208.

Bailey, C.H., Kandel, E.R., and Si, K. (2004). The persistence of long-term memory: a molecular approach to self-sustaining changes in learning-induced synaptic growth. Neuron *44*, 49–57.

Bhalla, U.S., and Iyengar, R. (1999). Emergent properties of networks of biological signaling pathways. Science *283*, 381–387.

Bonsi, P., De Persis, C., Calabresi, P., Bernardi, G., and Pisani, A. (2004). Coordinate high-frequency pattern of stimulation and calcium levels control the induction of LTP in striatal cholinergic interneurons. Learn. Mem. *11*, 755–760.

Bredt, D.S., and Nicoll, R.A. (2003). AMPA receptor trafficking at excitatory synapses. Neuron *40*, 361–379.

Chung, H.J., Steinberg, J.P., Huganir, R.L., and Linden, D.J. (2003). Requirement of AMPA receptor GluR2 phosphorylation for cerebellar long-term depression. Science *300*, 1751–1755.

Clark, J.D., Lin, L.L., Kriz, R.W., Ramesha, C.S., Sultzman, L.A., Lin, A.Y., Milona, N., and Knopf, J.L. (1991). A novel arachidonic acid-selective cytosolic PLA2 contains a Ca^{2+}-dependent translocation domain with homology to PKC and GAP. Cell *65*, 1043–1051.

Cobb, M.H., and Goldsmith, E.J. (1995). How MAP kinases are regulated. J. Biol. Chem. *270*, 14843–14846.

Corbit, K.C., Trakul, N., Eves, E.M., Diaz, B., Marshall, M., and Rosner, M.R. (2003). Activation of Raf-1 signaling by protein kinase C through a mechanism involving Raf kinase inhibitory protein. J. Biol. Chem. *278*, 13061–13068.

Cormier, R.J., Mauk, M.D., and Kelly, P.T. (1993). Glutamate iontophoresis induces long-term potentiation in the absence of evoked presynaptic activity. Neuron *10*, 907–919.

Cowley, S., Paterson, H., Kemp, P., and Marshall, C.J. (1994). Activation of MAP kinase kinase is necessary and sufficient for PC12 differentiation and for transformation of NIH 3T3 cells. Cell *77*, 841–852.

Crépel, F., and Jaillard, D. (1991). Pairing of pre- and postsynaptic activities in cerebellar Purkinje cells induces long-term changes in synaptic efficacy *in vitro*. J. Physiol. *432*, 123–141.

De Zeeuw, C.I., Hansel, C., Bian, F., Koekkoek, S.K., van Alphen, A.M., Linden, D.J., and Oberdick, J. (1998). Expression of a protein kinase C inhibitor in Purkinje cells blocks cerebellar LTD and adaptation of the vestibulo-ocular reflex. Neuron *20*, 495–508.

Eilers, J., Takechi, H., Finch, E.A., Augustine, G.J., and Konnerth, A. (1997). Local dendritic Ca^{2+} signaling induces cerebellar long-term depression. Learn. Mem. *4*, 159–168.

Endo, S., and Launey, T. (2003). ERKs regulate PKC-dependent synaptic depression and declustering of glutamate receptors in cerebellar Purkinje cells. Neuropharmacology *45*, 863–872.

Favata, M.F., Horiuchi, K.Y., Manos, E.J., Daulerio, A.J., Stradley, D.A., Feeser, W.S., Van Dyk, D.E., Pitts, W.J., Earl, R.A., Hobbs, F., et al. (1998). Identification of a novel inhibitor of mitogen-activated protein kinase kinase. J. Biol. Chem. *273*, 18623–18632.

Finch, E.A., and Augustine, G.J. (1998). Local calcium signalling by inositol-1,4,5-trisphosphate in Purkinje cell dendrites. Nature *396*, 753–756.

Franks, K.M., and Sejnowski, T.J. (2002). Complexity of calcium signaling in synaptic spines. Bioessays *24*, 1130–1144.

Gall, D., Prestori, F., Sola, E., D'Errico, A., Roussel, C., Forti, L., Rossi, P., and D'Angelo, E. (2005). Intracellular calcium regulation by burst discharge determines bidirectional long-term synaptic plasticity at the cerebellum input stage. J. Neurosci. *25*, 4813–4822.

Giese, K.P., Fedorov, N.B., Filipkowski, R.K., and Silva, A.J. (1998). Autophosphorylation at Thr286 of the alpha calcium-calmodulin kinase II in LTP and learning. Science *279*, 870–873.

Gordon, R.D., Leighton, I.A., Campbell, D.G., Cohen, P., Creaney, A., Wilton, D.C., Masters, D.J., Ritchie, G.A., Mott, R., Taylor, I.W., et al. (1996). Cloning and expression of cystolic phospholipase A2 (cPLA2) and a naturally occurring variant. Phosphorylation of Ser505 of recombinant cPLA2 by p42 mitogen-activated protein kinase results in an increase in specific activity. Eur. J. Biochem. *238*, 690–697.

Gustafsson, B., Wigstrom, H., Abraham, W.C., and Huang, Y.Y. (1987). Long-term potentiation in the hippocampus using depolarizing current pulses as the conditioning stimulus to single volley synaptic potentials. J. Neurosci. *7*, 774–780.

Hansel, C., de Jeu, M., Belmeguenai, A., Houtman, S.H., Buitendijk, G.H., Andreev, D., De Zeeuw, C.I., and Elgersma, Y. (2006). αCaMKII is essential for cerebellar LTD and motor learning. Neuron *51*, 835–843.

Hartell, N.A. (1994). cGMP acts within cerebellar Purkinje cells to produce long term depression via mechanisms involving PKC and PKG. Neuroreport *5*, 833–836.

Hartmann, J., and Konnerth, A. (2005). Determinants of postsynaptic Ca^{2+} signaling in Purkinje neurons. Cell Calcium *37*, 459–466.

Hirono, M., Sugiyama, T., Kishimoto, Y., Sakai, I., Miyazawa, T., Kishio, M., Inoue, H., Nakao, K., Ikeda, M., Kawahara, S., et al. (2001). Phospholipase Cβ4 and protein kinase Cα and/or protein kinase CβI are involved in the induction of long term depression in cerebellar Purkinje cells. J. Biol. Chem. *276*, 45236–45242.

Hockberger, P.E., Tseng, H.Y., and Connor, J.A. (1989). Fura-2 measurements of cultured rat Purkinje neurons show dendritic localization of Ca^{2+} influx. J. Neurosci. *9*, 2272–2284.

House, C., and Kemp, B.E. (1987). Protein kinase C contains a pseudosubstrate prototope in its regulatory domain. Science *238*, 1726–1728.

Humeau, Y., and Luthi, A. (2007). Dendritic calcium spikes induce bi-directional synaptic plasticity in the lateral amygdala. Neuropharmacology *52*, 234–243.

Inoue, T., Kato, K., Kohda, K., and Mikoshiba, K. (1998). Type 1 inositol 1,4,5-trisphosphate receptor is required for induction of long-term depression in cerebellar Purkinje neurons. J. Neurosci. *18*, 5366–5373.

Ito-Ishida, A., Kakegawa, W., and Yuzaki, M. (2006). ERK1/2 but not p38 MAP kinase is essential for the long-term depression in mouse cerebellar slices. Eur. J. Neurosci. *24*, 1617–1622.

Ito, M. (2001). Cerebellar long-term depression: characterization, signal transduction, and functional roles. Physiol. Rev. *81*, 1143–1195.

Jande, S.S., Maler, L., and Lawson, D.E. (1981). Immunohistochemical mapping of vitamin D-dependent calcium-binding protein in brain. Nature *294*, 765–767.

Kasono, K., and Hirano, T. (1994). Critical role of postsynaptic calcium in cerebellar long-term depression. Neuroreport *6*, 17–20.

Kauer, J.A., Malenka, R.C., and Nicoll, R.A. (1988). NMDA application potentiates synaptic transmission in the hippocampus. Nature *334*, 250–252.

Kawasaki, H., Fujii, H., Gotoh, Y., Morooka, T., Shimohama, S., Nishida, E., and Hirano, T. (1999). Requirement for mitogen-activated protein kinase in cerebellar long term depression. J. Biol. Chem. *274*, 13498–13502.

Khodakhah, K., and Armstrong, C.M. (1997). Induction of long-term depression and rebound potentiation by inositol trisphosphate in cerebellar Purkinje neurons. Proc. Natl. Acad. Sci. USA *94*, 14009–14014.

Köhler, T., Heinisch, M., Kirchner, M., Peinhardt, G., Hirschelmann, R., and Nuhn, P. (1992). Phospholipase A_2 inhibition by alkylbenzoylacrylic acids. Biochem. Pharmacol. *44*, 805–813.

Kondo, T., Kakegawa, W., and Yuzaki, M. (2005). Induction of long-term depression and phosphorylation of the δ2 glutamate receptor by protein kinase C in cerebellar slices. Eur. J. Neurosci. *22*, 1817–1820.

Konnerth, A., Dreessen, J., and Augustine, G.J. (1992). Brief dendritic calcium signals initiate long-lasting synaptic depression in cerebellar Purkinje cells. Proc. Natl. Acad. Sci. USA *89*, 7051–7055.

Kuroda, S., Schweighofer, N., and Kawato, M. (2001). Exploration of signal transduction pathways in cerebellar long-term depression by kinetic simulation. J. Neurosci. *21*, 5693–5702.

Leitges, M., Kovac, J., Plomann, M., and Linden, D.J. (2004). A unique PDZ ligand in PKCα confers induction of cerebellar long-term synaptic depression. Neuron *44*, 585–594.

Lev-Ram, V., Jiang, T., Wood, J., Lawrence, D.S., and Tsien, R.Y. (1997). Synergies and coincidence requirements between NO, cGMP, and Ca^{2+} in the induction of cerebellar long-term depression. Neuron *18*, 1025–1038.

Lin, L.L., Wartmann, M., Lin, A.Y., Knopf, J.L., Seth, A., and Davis, R.J. (1993). cPLA2 is phosphorylated and activated by MAP kinase. Cell *72*, 269–278.

Linden, D.J. (1994). Long-term synaptic depression in the mammalian brain. Neuron *12*, 457–472.

Linden, D.J. (1995). Phospholipase A2 controls the induction of short-term versus long-term depression in the cerebellar Purkinje neuron in culture. Neuron *15*, 1393–1401.

Linden, D.J. (1996). A protein synthesis-dependent late phase of cerebellar long-term depression. Neuron *17*, 483–490.

Linden, D.J., and Connor, J.A. (1991). Participation of postsynaptic PKC in cerebellar long-term depression in culture. Science *254*, 1656–1659.

Linden, D.J., Dickinson, M.H., Smeyne, M., and Connor, J.A. (1991). A long-term depression of AMPA currents in cultured cerebellar Purkinje neurons. Neuron *7*, 81–89.

Lisman, J., and Goldring, M. (1988). Evaluation of a model of long-term memory based on the properties of the Ca^{2+}/calmodulin-dependent protein kinase. J. Physiol. (Paris) *83*, 187–197.

Lisman, J., Schulman, H., and Cline, H. (2002). The molecular basis of CaMKII function in synaptic and behavioural memory. Nat. Rev. Neurosci. *3*, 175–190.

López-Nicolás, R., López-Andreo, M.J., Marín-Vicente, C., Gómez-Fernández, J.C., and Corbalán-García, S. (2006). Molecular mechanisms of PKCα localization and activation by arachidonic acid. The *C2* domain also plays a role. J. Mol. Biol. *357*, 1105–1120.

Malenka, R.C., and Bear, M.F. (2004). LTP and LTD: an embarrassment of riches. Neuron *44*, 5–21.

Malenka, R.C., Lancaster, B., and Zucker, R.S. (1992). Temporal limits on the rise in postsynaptic calcium required for the induction of long-term potentiation. Neuron *9*, 121–128.

Marais, R., Light, Y., Mason, C., Paterson, H., Olson, M.F., and Marshall, C.J. (1998). Requirement of Ras-GTP-Raf complexes for activation of Raf-1 by protein kinase C. Science *280*, 109–112.

Markevich, N.I., Tsyganov, M.A., Hoek, J.B., and Kholodenko, B.N. (2006). Long-range signaling by phosphoprotein waves arising from bistability in protein kinase cascades. Mol. Syst. Biol. *2*, 61.

Marriott, G., Roy, P., and Jacobson, K. (2003). Preparation and light-directed activation of caged proteins. Methods Enzymol. *360*, 274–288.

Miyata, M., Finch, E.A., Khiroug, L., Hashimoto, K., Hayasaka, S., Oda, S.I., Inouye, M., Takagishi, Y., Augustine, G.J., and Kano, M. (2000). Local calcium release in dendritic spines required for long-term synaptic depression. Neuron *28*, 233–244.

Muller, D., Buchs, P.A., Dunant, Y., and Lynch, G. (1990). Protein kinase C activity is not responsible for the expression of long-term potentiation in hippocampus. Proc. Natl. Acad. Sci. USA *87*, 4073–4077.

Murakami, K., and Routtenberg, A. (1985). Direct activation of purified protein kinase C by unsaturated fatty acids (oleate and arachidonate) in the absence of phospholipids and Ca2+. FEBS Lett. *192*, 189–193.

Murashima, M., and Hirano, T. (1999). Entire course and distinct phases of day-lasting depression of miniature EPSC amplitudes in cultured Purkinje neurons. J. Neurosci. *19*, 7326–7333.

Nevian, T., and Sakmann, B. (2006). Spine Ca^{2+} signaling in spike-timing-dependent plasticity. J. Neurosci. *26*, 11001–11013.

Newton, A.C. (2001). Protein kinase C: structural and spatial regulation by phosphorylation, cofactors, and macromolecular interactions. Chem. Rev. *101*, 2353–2364.

Nishida, E., and Gotoh, Y. (1993). The MAP kinase cascade is essential for diverse signal transduction pathways. Trends Biochem. Sci. *18*, 128–131.

Nishizuka, Y. (1995). Protein kinase C and lipid signaling for sustained cellular responses. FASEB J. *9*, 484–496.

Nordquist, D.T., Kozak, C.A., and Orr, H.T. (1988). cDNA cloning and characterization of three genes uniquely expressed in cerebellum by Purkinje neurons. J. Neurosci. *8*, 4780–4789.

Okazaki, K., and Sagata, N. (1995). MAP kinase activation is essential for oncogenic transformation of NIH3T3 cells by Mos. Oncogene *10*, 1149–1157.

Okubo, Y., Kakizawa, S., Hirose, K., and Iino, M. (2004). Cross talk between metabotropic and ionotropic glutamate receptor-mediated signaling in parallel fiber-induced inositol 1,4,5-trisphosphate production in cerebellar Purkinje cells. J. Neurosci. *24*, 9513–9520.

Oliet, S.H., Malenka, R.C., and Nicoll, R.A. (1997). Two distinct forms of long-term depression coexist in CA1 hippocampal pyramidal cells. Neuron *18*, 969–982.

Petrozzino, J.J., Pozzo Miller, L.D., and Connor, J.A. (1995). Micromolar Ca^{2+} transients in dendritic spines of hippocampal pyramidal neurons in brain slice. Neuron *14*, 1223–1231.

Reynolds, T., and Hartell, N.A. (2000). An evaluation of the synapse specificity of long-term depression induced in rat cerebellar slices. J. Physiol. *527*, 563–577.

Reynolds, T., and Hartell, N.A. (2001). Roles for nitric oxide and arachidonic acid in the induction of heterosynaptic cerebellar LTD. Neuroreport *12*, 133–136.

Sakurai, M. (1990). Calcium is an intracellular mediator of the climbing fiber in induction of cerebellar long-term depression. Proc. Natl. Acad. Sci. USA *87*, 3383–3385.

Sanhueza, M., McIntyre, C.C., and Lisman, J.E. (2007). Reversal of synaptic memory by Ca^{2+}/calmodulin-dependent protein kinase II inhibitor. J. Neurosci. *27*, 5190–5199.

Shinomura, T., Asaoka, Y., Oka, M., Yoshida, K., and Nishizuka, Y. (1991). Synergistic action of diacylglycerol and unsaturated fatty acid for protein kinase C activation: its possible implications. Proc. Natl. Acad. Sci. USA *88*, 5149–5153.

Shirai, Y., Kashiwagi, K., Yagi, K., Sakai, N., and Saito, N. (1998). Distinct effects of fatty acids on translocation of γ- and ε-subspecies of protein kinase C. J. Cell Biol. *143*, 511–521.

Si, K., Giustetto, M., Etkin, A., Hsu, R., Janisiewicz, A.M., Miniaci, M.C., Kim, J.H., Zhu, H., and Kandel, E.R. (2003). A neuronal isoform of CPEB regulates local protein synthesis and stabilizes synapse-specific long-term facilitation in aplysia. Cell *115*, 893–904.

Steinberg, J.P., Takamiya, K., Shen, Y., Xia, J., Rubio, M.E., Yu, S., Jin, W., Thomas, G.M., Linden, D.J., and Huganir, R.L. (2006). Targeted in vivo mutations of the AMPA receptor subunit GluR2 and its interacting protein PICK1 eliminate cerebellar long-term depression. Neuron *49*, 845–860.

Tanaka, K., Khiroug, L., Santamaria, F., Doi, T., Ogasawara, H., Ellis-Davies, G.C., Kawato, M., and Augustine, G.J. (2007). Ca^{2+} requirements for cerebellar long-term synaptic depression: role for a postsynaptic leaky integrator. Neuron *54*, 787–800.

Tanoue, T., and Nishida, E. (2003). Molecular recognitions in the MAP kinase cascades. Cell. Signal. *15*, 455–462.

Tatsukawa, T., Chimura, T., Miyakawa, H., and Yamaguchi, K. (2006). Involvement of basal protein kinase C and extracellular signal-regulated kinase 1/2 activities in constitutive internalization of AMPA receptors in cerebellar Purkinje cells. J. Neurosci. *26*, 4820–4825.

Tsuruno, S., and Hirano, T. (2007). Persistent activation of protein kinase Cα is not necessary for expression of cerebellar long-term depression. Mol. Cell. Neurosci. *35*, 38–48.

Wang, S.S., and Augustine, G.J. (1995). Confocal imaging and local photolysis of caged compounds: dual probes of synaptic function. Neuron *15*, 755–760.

Wang, Y.T., and Linden, D.J. (2000). Expression of cerebellar long-term depression requires postsynaptic clathrin-mediated endocytosis. Neuron *25*, 635–647.

Wang, S.S., Denk, W., and Hausser, M. (2000a). Coincidence detection in single dendritic spines mediated by calcium release. Nat. Neurosci. *3*, 1266–1273.

Wang, S.S., Khiroug, L., and Augustine, G.J. (2000b). Quantification of spread of cerebellar long-term depression with chemical two-photon uncaging of glutamate. Proc. Natl. Acad. Sci. USA *97*, 8635–8640.

Wen-Sheng, W. (2006). Protein kinase C α trigger Ras and Raf-independent MEK/ERK activation for TPA-induced growth inhibition of human hepatoma cell HepG2. Cancer Lett. *239*, 27–35.

Yang, S.N., Tang, Y.G., and Zucker, R.S. (1999). Selective induction of LTP and LTD by postsynaptic $[Ca^{2+}]_i$ elevation. J. Neurophysiol. *81*, 781–787.

Zheng, Y., Liu, H., Coughlin, J., Zheng, J., Li, L., and Stone, J.C. (2005). Phosphorylation of RasGRP3 on threonine 133 provides a mechanistic link between PKC and Ras signaling systems in B cells. Blood *105*, 3648–3654.

Zucker, R.S., and Regehr, W.G. (2002). Short-term synaptic plasticity. Annu. Rev. Physiol. *64*, 355–405.